Laimer D,Dolznig H,Kollmann K,Vesely PW,Schlederer M,Merkel O,Schiefer AI,Hassler MR,Heider S,Amenitsch L,Thallinger C,Staber PB,Simonitsch-Klupp I,Artaker M,Lagger S,Turner SD,Pileri S,Piccaluga PP,Valent P,Messana K,Landra I,Weichhart T,Knapp S,Shehata M,Todaro M,Sexl V,Hofler G,Piva R,Medico E,Ruggeri BA,Cheng M,Eferl R,Egger G,Penninger JM,Jaeger U,Moriggl R,Inghirami G,Kenner L

PDGFR blockade is a rational and effective therapy for NPM-ALK-driven lymphomas.

NATURE MEDICINE (2012) 18

DOI: 10.1038/nm.2966

Identification of PDGFR blockade as a rational and highly effective therapy for NPM-ALK driven lymphomas

Daniela Laimer[1#], Helmut Dolznig[2#], Karoline Kollmann[3#], Paul W. Vesely[4#], Michaela Schlederer[5], Olaf Merkel[6], Ana-Iris Schiefer[1], Melanie R. Hassler[1,7], Susi Heider[1], Lena Amenitsch[1], Christiane Thallinger[7], Philipp B. Staber[8,9], Ingrid Simonitsch-Klupp[1], Matthias Artaker[10], Sabine Lagger[11], Stefano Pileri[12], Pier Paolo Piccaluga[12], Peter Valent[13,14], Katia Messana[15], Indira Landra[15], Thomas Weichhart[2], Sylvia Knapp[16], Medhat Shehata[13], Maria Todaro[15], Veronika Sexl[4], Gerald Höfler[3], Roberto Piva[15,17], Enzo Medico[18], Robert Eferl[19], Gerda Egger[1], Josef M. Penninger[20], Ulrich Jaeger[13], Richard Moriggl[5], Giorgio Inghirami[15,17] and Lukas Kenner[1,5*]

[1]Clinical Institute of Clinical Pathology, Medical University of Vienna, Vienna, Austria.
[2]Institute of Medical Genetics, Medical University of Vienna, Vienna, Austria.
[3]Institute of Pharmacology and Toxicology, Veterinary University Vienna, Vienna, Austria.
[4]Institute of Pathology, Medical University Graz, Graz, Austria; current address: The Scripps Research Institute, La Jolla, CA.
[5]Ludwig Boltzmann Institute for Cancer Research (LBI-CR), Vienna, Austria.
[6]Laboratory for Immunological and Molecular Cancer Research, 3rd Medical Department of the Paracelsus Medical University, Salzburg, Austria.
[7]Department of Internal Medicine I, Division of Oncology, Medical University of Vienna, Vienna, Austria.
[8]Division of Hematology, Medical University Graz, Graz, Austria.
[9]Harvard Stem Cell Institute, Harvard Medical School, Boston, MA, USA.
[10]Department o Molecular Genetics, MFPL, Medical University of Vienna, Vienna, Austria.
[11]Welcome Trust Centre for Cell Biology, University of Edinburgh, Edinburgh, UK.
[12]Chair of Pathology and Hematopathology Unit, Department of Hematology and Oncology "L. and A. Seràgnoli", S. Orsola-Malpighi Hospital, University of Bologna, Bologna, Italy.
[13]Department of Internal Medicine I, Division of Hematology and Hemostaseology, Comprehensive Cancer Center CCC/Drug & Target Screening Unit DTSU, Medical University of Vienna, Vienna, Austria.
[14]Ludwig Boltzmann Cluster Oncology, Vienna, Austria.
[15]Department of Biomedical Sciences and Human Oncology, Center for Experimental Research and Medical Studies, University of Torino, Turin, Italy.
[16]Center for Molecular Medicine of the Austrian Academy of Sciences & Department of Medicine I, Division of Infectious Diseases and Tropical Medicine, Medical University of Vienna, Vienna, Austria.
[17]Department of Pathology, and NYU Cancer Center, New York University School of Medicine, New York, NY, USA.
[18]Laboratory of Functional Genomics, Institute for Cancer Research and Treatment, University of Torino, Turin, Italy.
[19]Institute for Cancer Research (ICR), Comprehensive Cancer Center (CCC), Medical University of Vienna, Vienna, Austria.
[20]IMBA, Institute of Molecular Biotechnology of the Austrian Academy of Science, Vienna, Austria.

[#]contributed equally
[*]corresponding author

Abstract

Anaplastic Large Cell Lymphoma (ALCL) is a Non-Hodgkin lymphoma found in children and young adults with poor survival rates. ALCLs frequently carry a chromosomal translocation that results in expression of the oncoprotein nucleophosmin-anaplastic lymphoma kinase (NPM-ALK). The key molecular downstream events required for NPM-ALK triggered lymphoma growth are still not entirely clear. Here we show that the AP-1 proteins cJun and JunB promote lymphoma development and tumor dissemination in a murine NPM-ALK lymphomagenesis model via transcriptional regulation of PDGFRB. Therapeutic inhibition of PDGFRB markedly prolonged survival of NPM-ALK transgenic mice and increased the efficacy of an ALK-specific inhibitor in transplanted NPM-ALK tumors. Remarkably, inhibition of PDGFRs in a late stage patient with refractory NPM-ALK-positive ALCL resulted in complete and sustained remission within 10 days of treatment. Our data identify PDGFRB as novel cJun/JunB target that could be utilized for a highly effective therapy to cure ALCL.

ALCLs are T-cell lymphomas[1,2] that comprise 10-20% of all Non-Hodgkin's lymphoma cases in children and 3% in adults[3]. About half of ALCL cases are positive for NPM-ALK fusion proteins caused by t(2;5)(p23;q35) translocation[4]. ALK translocations or point mutations have also been described in DLBCLs (diffuse large B-cell lymphomas) and in several non-lymphoid neoplasms[5-8]. Inhibition of ALK fusion proteins by specific compounds such as crizotinib showed promising clinical responses in ALCL and NSCLC (non-small cell lung cancer)[9,10]. However, ALK mutations conferring resistance to crizotinib have also been reported[11].

Recent studies have linked NPM-ALK expression to induction of AP-1 transcription factors JunB and cJun[12,13]. To investigate their role in NPM-ALK-driven T-cell lymphomas, we conditionally deleted cJun and/or JunB in T-cells of transgenic mice carrying the human NPM-ALK fusion-tyrosine-kinase under the control of the murine CD4-promotor[14] (*CD4*-NPM-ALK) (Fig. 1a). Gene deletion was confirmed by DNA genotyping (data not shown), real-time PCR, Western blotting and immunohistochemistry (IHC) (Suppl. Fig. S1a-c). Expression of oncogenic NPM-ALK in T-cells was not affected by Jun deletion (Suppl. Fig. S1a-c) and all genetic cohorts displayed normal T-cell development before lymphoma onset (Suppl. Fig. S1d,e; data not shown). As expected, *CD4*-NPM-ALK mice developed T-cell lymphomas around 8 weeks after birth[14]. The overall survival was not affected by deletion of individual Jun proteins (Fig.1b), however, inactivation of both, cJun and JunB, in *CD4*-NPM-ALK-*CD4*$^{\Delta\Delta Jun}$ mice resulted in significantly prolonged survival (Fig. 1b). *CD4*-NPM-ALK-*CD4*$^{\Delta\Delta Jun}$ lymphomas showed markedly reduced proliferation and significantly increased apoptosis when compared to *CD4*-NPM-ALK lymphomas (Fig. 1c; Suppl. Fig. S2a,b). Consistently, *CD4*-NPM-ALK-*CD4*$^{\Delta\Delta Jun}$ but not *CD4*-NPM-ALK lymphoma cells failed to grow *in vitro* (data not shown) and CRE-mediated deletion of cJun/JunB in established *CD4*-NPM-ALK-cJun$^{flox/flox}$;JunB$^{flox/flox}$ cell lines induced cell death (Suppl. Fig. S2c). However, freshly isolated *CD4*-NPM-ALK-*CD4*$^{\Delta\Delta Jun}$ lymphoma cells formed palpable tumors when engrafted into SCID mice, albeit after a long latency (Suppl. Fig. S2d). These data demonstrate that cJun and JunB are critical regulators of NPM-ALK driven T-cell lymphoma development.

T-cell lymphomas spread to many organs in *CD4*-NPM-ALK transgenic mice[14]. Although *CD4*-NPM-ALK-*CD4*$^{\Delta\Delta Jun}$ mice eventually developed lymphomas, we failed to detect dissemination of tumor cells (Fig. 1d,e; Suppl. Fig. S2e). Importantly, blood vessel numbers were significantly decreased in primary lymphomas of *CD4*-NPM-ALK-*CD4*$^{\Delta\Delta Jun}$ when compared to *CD4*-NPM-ALK controls (Fig. 2a). Surprisingly, expression and activation of the mural pericyte cell marker PDGFRB (platelet derived growth factor receptor beta) was readily detectable in lymphoma cells of *CD4*-NPM-ALK mice but essentially absent in T-cell lymphomas of *CD4*-NPM-ALK-*CD4*$^{\Delta\Delta Jun}$ mice (Fig. 2b,c). Tumor cells from single *CD4*-NPM-ALK-*CD4*$^{\Delta JunB}$ and *CD4*-NPM-ALK-*CD4*$^{\Delta cJun}$ mice displayed intermediate PDGFRB protein

expression (Suppl. Fig. S3a). PDGFRB mRNA expression was also decreased in lymphomas of *CD4*-NPM-ALK-*CD4*$^{\Delta\Delta Jun}$ mice when compared to *CD4*-NPM-ALK lymphomas (Fig. 2d) suggesting a transcriptional regulation of PDGFRB by Jun proteins. Consistently, AP-1 consensus sequences were identified within the murine PDGFRB promoter and first intron that were conserved among other species (Suppl. Fig. S3b,c)[15,16]. Moreover, analysis of ENCODE transcription factor binding tracks revealed binding of cJun and JunB to the PDGFRB intronic AP-1 site in the human K562 leukemia cell line (Suppl. Fig. S3d)[15,17]. EMSA analysis of nuclear extracts from NPM-ALK lymphomas demonstrated AP-1 DNA binding to the consensus sequence, which was reduced after antibody-mediated cJun and JunB depletion (Fig. 2e). Moreover, cJun/JunB binding to the PDGFRB promoter was confirmed by Chromatin Immunoprecipitation (ChIP) assays of human dermal fibroblasts (Fig. 2f), murine NPM-ALK cell lines and tumor tissues (Suppl. Fig S3e,f) as well as luciferase reporter assays in Jurkat cells (Fig. 2g) or in HeLa cells using PDGFRB promoter constructs with and without an AP-1 site (Suppl. Fig. S3g). These data demonstrate transcriptional regulation of PDGFRB by cJun and JunB.

PDGFRs have not been implicated in ALCL but are known physiologic regulators of tumor growth[18-20]. We therefore investigated the effects of the PDGFR kinase inhibitor imatinib on established murine lymphoma cell lines. Imatinib also blocks BCR-ABL, KIT and PDGFRA activity with high affinity[21], but has no effect on ALK[22,23]. The NPM-ALK lymphoma cell lines lacked BCR-ABL (data not shown) and PDGFRA expression whereas KIT was expressed at variable levels (Fig. 3a, Suppl. Fig. S4a,b). PDGFRB expression ranged from high to non-detectable levels (Figure 3a; Suppl. Fig. S4a). The effects of imatinib on tumor growth were then evaluated in tumor cell transplantation experiments. Importantly, imatinib treatment of tumor bearing mice resulted in markedly reduced tumor growth (Fig. 3b; Suppl. Fig. S4c). The response rate of individual transplanted cell lines correlated with the level of PDGFRB expression since A333-derived lymphomas (lack PDGFRB but express high levels of c-Kit) were not affected by imatinib treatment (Fig. 3b). Similar results were obtained using nilotinib (Suppl. Fig. S4d), another PDGFRB kinase inhibitor[24,25]. Neither expression of cytokines and their receptors implicated in ALCL lymphomagenesis such as IL-9 and IL-22[26,27] (Suppl. Fig. S4e), nor peripheral and splenic T-cell populations (Suppl. Fig. S5a-c) or tumor infiltrating T subsets (Suppl. Fig S5d,e) were affected by imatinib treatment. These data demonstrate that inhibition of PDGFRB markedly impairs growth of transplanted ALCL tumor cells.

We next explored the effects of imatinib on primary lymphomas in *CD4*-NPM-ALK mice. Imatinib treatment significantly increased overall survival (Fig. 3c), reduced *in vivo* tumor cell proliferation and enhanced apoptosis (Fig. 3d). Imatinib also blocked proliferation and enhanced cell death of murine PDGFRB^{+} lymphoma cell lines *in vitro* (Suppl. Fig. S6a,b). As expected, imatinib reduced PDGFRB phosphorylation in *CD4*-NPM-ALK cell lines (Suppl.

Fig. S6c) and in tumor tissues of *CD4*-NPM-ALK mice (Fig. 3e) resulting in blunted AKT and STAT3 but not ERK phosphorylation (Suppl. Fig. S6d,e). Moreover, PDGFRB phosphorylation of PDGFB-stimulated lymphoma cells was impaired by imatinib in a dose dependent manner (Suppl. Fig. S6f,g), resulting in reduced proliferation (Suppl. Fig. S6h). Imatinib also reduced PDGFB mRNA levels (Suppl. Fig. S6i) in *CD4*-NPM-ALK lymphomas, indicating an autoregulatory PDGF secretion loop. Remarkably, imatinib-treated *CD4*-NPM-ALK-*CD4*$^{\Delta\Delta Jun}$ mice did not develop tumors during the 30 week observation period (Fig. 3c) and tumor cell dissemination to distant organs was completely blocked (Suppl. Fig. S7a). This is most likely due to an additional effect of imatinib on the tumor stroma as also reported for other cancers[28,29] (Suppl. Fig. S7b-f).

We next tested imatinib in combination with the ALK inhibitor crizotinib[9]. Imatinib and crizotinib synergistically reduced tumor growth of grafted NPM-ALK$^+$ lymphomas (Fig. 3f). Similar results were obtained with the ALK inhibitor CEP28122[30]. Moreover, imatinib reduced growth and percentage of lymphomas that relapsed after CEP28122 treatment (Fig. 3g,h). These data demonstrate that therapeutic blockade of PDGFRs can markedly alleviate relapse of ALCLs after ALK inhibition.

The vast majority of human NPM-ALK$^+$ and NPM-ALK$^-$ ALCLs expressed high levels of JunB, cJun, PDGFRA and PDGFRB mRNA [31-34] (Fig. 4a) and protein (Fig. 4b; Suppl. Fig. S8a,b). Consistently, two highly conserved AP-1 binding sites were identified in the human PDGFRA promoter (Suppl. Fig. S8c). KIT and BCR-ABL protein expression as well as KIT mutations were not detected (Suppl. Fig. S8d; data not shown). In contrast to lymphomas, established human ALK$^+$ ALCL cell lines were negative for PDGFRA/B (Suppl. Fig. S8e) and ALK expression was required to maintain JunB mRNA expression (Suppl. Fig. S8f). Our data demonstrate that ALK$^+$ human ALCLs express high levels of PDGFRA/B and JunB.

Based on our results, we obtained ethical approval and informed consent to perform imatinib treatment of an ALCL patient with very poor prognosis. The patient suffered from NPM-ALK$^+$, JunB$^+$, cJun$^+$, PDGFRA$^+$, PDGFRB$^+$, c-Kit$^-$ ALCL (Fig. 4c) that was refractory to conventional first line chemotherapy and had relapsed after autologous stem cell transplantation. Amazingly, the patient was in complete clinical remission with reduced tumor markers and normalized PDGFB levels within 10-14 days of imatinib therapy (Fig. 4d,e,f,g). Of note, we also observed high PDGFB levels in the serum of four additional ALCL patients (Suppl. Fig. S8g). The patient has now been free of ALCL since 18 months after initiation of imatinib therapy. These data demonstrate rapid and complete remission of ALCL in a terminally sick patient without other treatment options.

Here we present evidence that JunB and cJun are crucial for growth and metastasis of ALCL lymphomas via regulation of PDGFR expression. PDGFR is not expressed in non-transformed T-cells and oncogenic NPM-ALK signaling might operate synergistically with

cJun/JunB to induce PDGFR. Mechanistically, PDGFR might promote ALCL formation by a combined effect on lymphoma cells and tumor stroma. Regulation of PDGFR in the tumor stroma and the qualitative contribution of stromal effects to drug responses observed in the mouse models used have to be further evaluated. Most importantly, imatinib treatment of a terminally ill patient, who was already refractory to conventional therapies, resulted in a complete disease remission demonstrating that ALCL can be cured. Our data also identified PDGFR inhibition as effective treatment option for tumors that have relapsed after ALK inhibition therapy. A clinical trial based on PDGFR expression in tumors is currently designed to enroll patients for second line ALCL.

Methods Summary

Mice carrying the human NPM-ALK fusion-gene were crossed with mice carrying a *CD4*-Cre as well as floxed alleles for JunB and/or cJun. Transplant experiments with *CD4*-NPM-ALK cell lines were performed using SCID mice followed by single or combination treatments with imatinib, nilotinib, and/or crizotinib. Balb/c ALK^+ ALCL cells were implanted into syngeneic Balb/c mice and recipients were treated with CEP28122 or CEP28122 + imatinib. Patient formalin fixed paraffin embedded tissues samples were kindly provided by the Clinical Institute of Pathology at the Medical University of Vienna after receipt of informed patient consent and in accordance with the declaration of Helsinki. Immunostainings were quantified with the HistoQuest™ and TissueQuest™ software. Western blot analyses were performed using total protein extracts. Chromatin Immunoprecipitation (ChIP) was executed with either 10^7 cells or 100 µg of tumor tissue from NPM-ALK lymphomas with and without cJun and/or JunB. Luciferase assays were performed using OneGlo and BetaGlo systems (Promega). For Electro Mobility Shift Assay (EMSA), cell lysates of NPM-ALK-positive mouse tumors were used. Supershift reactions of AP-1 complexes were performed using antibodies specific for cJun and JunB. After ethical approval and informed consent, an ALCL patient was treated with 400 mg imatinib/day. Platelet-low plasma samples were collected from the ALCL patient before and after imatinib treatment and analyzed for CRP, haptoglobin (HP), soluble CD30 (sTNFRSF8), beta-2-microglobulin (B2M), and PDGFB levels by ELISA. The statistical analyses were performed using GraphPad Prism 5 software. The raw data were analyzed with either ANOVA and the Tukey Post test or with the Student's t-test.

Author Contributions: H.D., P.W.V, O.M., P.V., T.W., M.S., V.S., G.H., G.E., J.M.P., U.J., R.M., G.I., R.E., L.K. designed experiments. D.L., H.D., K.K, P.W.V, M.S., O.M., A.I.S., M.R.H., S.H., L.A., C.T., P.S., I.S., M.A., S.P., P.P.P., K.M., I.L., S.K., M.S., M.T., S.L., R.P., E.M., G.E., R.M. performed experiments and collected and analyzed data. H.D., V.S., R.M.,

J.M.P., G.I., R.E. and L.K. wrote the manuscript. All authors discussed the results and edited the manuscript.

Competing financial interests

The authors declare no competing financial interests.

References

1. Kadin, M.E. Ki-1/CD30+ (anaplastic) large-cell lymphoma: maturation of a clinicopathologic entity with prospects of effective therapy. *Journal of clinical oncology : official journal of the American Society of Clinical Oncology* **12**, 884-887 (1994).
2. Kadin, M.E. Primary Ki-1-positive anaplastic large-cell lymphoma: a distinct clinicopathologic entity. *Ann Oncol* **5 Suppl 1**, 25-30 (1994).
3. Stein, H.*, et al.* CD30(+) anaplastic large cell lymphoma: a review of its histopathologic, genetic, and clinical features. *Blood* **96**, 3681-3695 (2000).
4. Morris, S.W.*, et al.* Fusion of a kinase gene, ALK, to a nucleolar protein gene, NPM, in non-Hodgkin's lymphoma. *Science* **263**, 1281-1284 (1994).
5. Chen, Y.*, et al.* Oncogenic mutations of ALK kinase in neuroblastoma. *Nature* **455**, 971-974 (2008).
6. George, R.E.*, et al.* Activating mutations in ALK provide a therapeutic target in neuroblastoma. *Nature* **455**, 975-978 (2008).
7. Janoueix-Lerosey, I.*, et al.* Somatic and germline activating mutations of the ALK kinase receptor in neuroblastoma. *Nature* **455**, 967-970 (2008).
8. Soda, M.*, et al.* Identification of the transforming EML4-ALK fusion gene in non-small-cell lung cancer. *Nature* **448**, 561-566 (2007).
9. Gambacorti-Passerini, C., Messa, C. & Pogliani, E.M. Crizotinib in anaplastic large-cell lymphoma. *N Engl J Med* **364**, 775-776 (2011).
10. Kwak, E.L.*, et al.* Anaplastic lymphoma kinase inhibition in non-small-cell lung cancer. *N Engl J Med* **363**, 1693-1703 (2010).
11. Choi, Y.L.*, et al.* EML4-ALK mutations in lung cancer that confer resistance to ALK inhibitors. *N Engl J Med* **363**, 1734-1739 (2010).
12. Mathas, S.*, et al.* Aberrantly expressed c-Jun and JunB are a hallmark of Hodgkin lymphoma cells, stimulate proliferation and synergize with NF-kappa B. *EMBO J* **21**, 4104-4113 (2002).
13. Staber, P.B.*, et al.* The oncoprotein NPM-ALK of anaplastic large-cell lymphoma induces JUNB transcription via ERK1/2 and JunB translation via mTOR signaling. *Blood* **110**, 3374-3383 (2007).
14. Chiarle, R.*, et al.* NPM-ALK transgenic mice spontaneously develop T-cell lymphomas and plasma cell tumors. *Blood* **101**, 1919-1927 (2003).
15. Kent, W.J.*, et al.* The human genome browser at UCSC. *Genome Res* **12**, 996-1006 (2002).
16. Cartharius, K.*, et al.* MatInspector and beyond: promoter analysis based on transcription factor binding sites. *Bioinformatics* **21**, 2933-2942 (2005).
17. Gertz, J.*, et al.* Analysis of DNA methylation in a three-generation family reveals widespread genetic influence on epigenetic regulation. *PLoS Genet* **7**, e1002228 (2011).
18. Andrae, J., Gallini, R. & Betsholtz, C. Role of platelet-derived growth factors in physiology and medicine. *Genes Dev* **22**, 1276-1312 (2008).

19. Claesson-Welsh, L. Signal transduction by the PDGF receptors. *Prog Growth Factor Res* **5**, 37-54 (1994).
20. Nissen, L.J*., et al.* Angiogenic factors FGF2 and PDGF-BB synergistically promote murine tumor neovascularization and metastasis. *The Journal of clinical investigation* **117**, 2766-2777 (2007).
21. Pardanani, A. & Tefferi, A. Imatinib targets other than bcr/abl and their clinical relevance in myeloid disorders. *Blood* **104**, 1931-1939 (2004).
22. Ergin, M*., et al.* Inhibition of tyrosine kinase activity induces caspase-dependent apoptosis in anaplastic large cell lymphoma with NPM-ALK (p80) fusion protein. *Exp Hematol* **29**, 1082-1090 (2001).
23. Gunby, R.H*., et al.* Structural insights into the ATP binding pocket of the anaplastic lymphoma kinase by site-directed mutagenesis, inhibitor binding analysis, and homology modeling. *J Med Chem* **49**, 5759-5768 (2006).
24. Hantschel, O., Rix, U. & Superti-Furga, G. Target spectrum of the BCR-ABL inhibitors imatinib, nilotinib and dasatinib. *Leuk Lymphoma* **49**, 615-619 (2008).
25. Stover, E.H*., et al.* The small molecule tyrosine kinase inhibitor AMN107 inhibits TEL-PDGFRbeta and FIP1L1-PDGFRalpha in vitro and in vivo. *Blood* **106**, 3206-3213 (2005).
26. Qiu, L*., et al.* Autocrine release of interleukin-9 promotes Jak3-dependent survival of ALK+ anaplastic large-cell lymphoma cells. *Blood* **108**, 2407-2415 (2006).
27. Savan, R*., et al.* A novel role for IL-22R1 as a driver of inflammation. *Blood* **117**, 575-584 (2011).
28. Pietras, K*., et al.* Inhibition of PDGF receptor signaling in tumor stroma enhances antitumor effect of chemotherapy. *Cancer Res* **62**, 5476-5484 (2002).
29. Sumida, T*., et al.* Anti-stromal therapy with imatinib inhibits growth and metastasis of gastric carcinoma in an orthotopic nude mouse model. *Int J Cancer* **128**, 2050-2062 (2011).
30. Cheng, M*., et al.* CEP-28122, a highly potent and selective orally active inhibitor of anaplastic lymphoma kinase with antitumor activity in experimental models of human cancers. *Mol Cancer Ther* **11**, 670-679 (2012).
31. Iqbal, J*., et al.* Molecular signatures to improve diagnosis in peripheral T-cell lymphoma and prognostication in angioimmunoblastic T-cell lymphoma. *Blood* **115**, 1026-1036 (2010).
32. Piccaluga, P.P*., et al.* Gene expression analysis of peripheral T cell lymphoma, unspecified, reveals distinct profiles and new potential therapeutic targets. *The Journal of clinical investigation* **117**, 823-834 (2007).
33. Eckerle, S*., et al.* Gene expression profiling of isolated tumour cells from anaplastic large cell lymphomas: insights into its cellular origin, pathogenesis and relation to Hodgkin lymphoma. *Leukemia : official journal of the Leukemia Society of America, Leukemia Research Fund, U.K* **23**, 2129-2138 (2009).
34. Piva, R*., et al.* Gene expression profiling uncovers molecular classifiers for the recognition of anaplastic large-cell lymphoma within peripheral T-cell neoplasms. *Journal of clinical oncology : official journal of the American Society of Clinical Oncology* **28**, 1583-1590 (2010).
35. Lee, P.P*., et al.* A critical role for Dnmt1 and DNA methylation in T cell development, function, and survival. *Immunity* **15**, 763-774 (2001).
36. Behrens, A*., et al.* Impaired postnatal hepatocyte proliferation and liver regeneration in mice lacking c-jun in the liver. *EMBO J* **21**, 1782-1790 (2002).
37. Kenner, L*., et al.* Mice lacking JunB are osteopenic due to cell-autonomous osteoblast and osteoclast defects. *J Cell Biol* **164**, 613-623 (2004).

38. Ovcharenko, I., Nobrega, M.A., Loots, G.G. & Stubbs, L. ECR Browser: a tool for visualizing and accessing data from comparisons of multiple vertebrate genomes. *Nucleic Acids Res* **32**, W280-286 (2004).
39. Gal-Yam, E.N.*, et al.* Frequent switching of Polycomb repressive marks and DNA hypermethylation in the PC3 prostate cancer cell line. *Proc Natl Acad Sci U S A* **105**, 12979-12984 (2008).
40. Pflegerl, P.*, et al.* Epidermal loss of JunB leads to a SLE phenotype due to hyper IL-6 signaling. *Proc Natl Acad Sci U S A* **106**, 20423-20428 (2009).

Acknowledgements

LK is supported by the „Fonds zur Förderung der wissenschaftlichen Forschung“ (FWF, P-18478-B12) and the Genome Research-Austria project “Inflammobiota”. RM, VS and RE are supported by the FWF (SFB-F28), VS is supported by FWF project 19723. GE is supported by an Elise Richter fellowship (FWF V102-B12) and an FP7 Marie Curie International Reintegration Grant (IRG 230984). HD is supported by the Herzfelder Family Foundation and the NOE Forschungs- und Bildungsges.m.b.H. PWV and PBS were supported by Jubiläumsfonds of the Austrian Nationalbank (P-12147). TW is supported by the Else-Kröner Fresensius Stiftung. SP and GI are supported by AIRC grant 5x1000 N. 10007 and GI by the ImmOnc grant (Piattaforme Tecnologiche BIO LR 34/2004). R.E. is supported by the FWF Doktoratskolleg-plus grant “Inflammation and Immunity”, the Comprehensive Cancer Center (CCC) Vienna Research Grant and the Austrian Federal Ministry of Science and Research GENAU grant“ Austromouse. J.M.P. is supported by the Austrian Academy of Sciences and an advanced ERC grant. The study was performed on behalf of the European Research Initiative on ALCL (ERIA). We thank Erwin F. Wagner for providing the $JunB^{flox/flox}$ and $cJun^{flox/flox}$ mice. We thank Drs. Cheng and Ruggeri from Cephalon for providing the CEP inhibitor. We thank Arne Ostman for helpful discussions and technical help with PDGFRB analysis and Sonja Reichmann for technical help with sCD30 and PDGFB assays.

Figure Legends

Figure 1. **JunB and cJun control survival and spreading of NPM-ALK lymphomas.**

(**a**) Mouse strains with T-cell-specific *CD4*-NPM-ALK expression and T-cell-specific deletion of either JunB (*CD4*-NPM-ALK-*CD4*-JunB$^{\Delta/\Delta}$;cJun$^{\Delta/+}$*;* designated *CD4*-NPM-ALK-*CD4*$^{\Delta JunB}$), cJun (*CD4*-NPM-ALK-*CD4*-cJun$^{\Delta/\Delta}$;JunB$^{\Delta/+}$*;* designated *CD4*-NPM-ALK-*CD4*$^{\Delta cJun}$), or both (*CD4*-NPM-ALK-*CD4*-cJun$^{\Delta/\Delta}$;JunB$^{\Delta/\Delta}$; designated *CD4*-NPM-ALK-*CD4*$^{\Delta\Delta Jun}$) were generated. (**b**) Kaplan-Meier curves depicting overall survival of *CD4*-NPM-ALK mice carrying deletion of JunB, cJun or both. Isogenic wild type mice are shown as control. (**c**) Sections of *CD4*-NPM-ALK and *CD4*-NPM-ALK-*CD4*$^{\Delta\Delta Jun}$ lymphomas were TUNEL-stained and Ki67-stained to assess apoptosis and proliferation, respectively. The mean number of TUNEL- and Ki67-positive cells among 2000 cells/tumor sample were determined using TissueQuest^{TM} software. Data from 5 different mice (mean value +/- SD) are shown. (**d**) H&E-staining of lymphoma and liver tissues of *CD4*-NPM-ALK and *CD4*-NPM-ALK-*CD4*$^{\Delta\Delta Jun}$ mice. While lymphomas are morphologically similar in both genotypes, there is a massive invasion of tumor cells into the liver of *CD4*-NPM-ALK mice (green arrowheads), which have already largely destroyed the liver architecture around the blood vessels (red asterisk). In contrast, no disseminated tumor cells were detectable in the liver of *CD4*-NPM-ALK-*CD4*$^{\Delta\Delta Jun}$ mice (red asterisk denotes blood vessel). **(e)** Periodic acid-Schiff (PAS)-stained livers of *CD4*-NPM-ALK and *CD4*-NPM-ALK-*CD4*$^{\Delta\Delta Jun}$ (small inset) mice. Tumor cells are clearly visible in the liver parenchyma (green arrowheads) of *CD4*-NPM-ALK mice whereas livers of *CD4*-NPM-ALK-*CD4*$^{\Delta\Delta Jun}$ mice were free of migrating tumor cells. Red asterisks denote blood vessels.

Figure 2. PDGFRB is a direct transcriptional target of JunB and cJun.

(**a**) CD31-immunostaining to detect blood vessels in *CD4*-NPM-ALK and *CD4*-NPM-ALK-*CD4*$^{\Delta\Delta Jun}$ lymphomas. Quantitative assessment using HistoQuest^{TM} software of the areas indicates a significant increase in vascularization in *CD4*-NPM-ALK lymphomas (n = 3). Data are mean values +/- SD. (**b**) PDGFRB and phospho-PDGFRB (pPDGFRB) expression in *CD4*-NPM-ALK and *CD4*-NPM-ALK-*CD4*$^{\Delta\Delta Jun}$ lymphomas. Wild type thymus is shown as a negative control. Insets show high magnification (600x). (**c**) Western blot analysis of PDGFRB expression in *CD4*-NPM-ALK and *CD4*-NPM-ALK-*CD4*$^{\Delta\Delta Jun}$ lymphomas. Expression of β-actin (ACTB) is shown as control. (**d**) PDGFRB mRNA levels are reduced in *CD4*-NPM-ALK-*CD4*$^{\Delta\Delta Jun}$ tumors when compared to *CD4*-NPM-ALK tumors (n = 3). PDGFRB mRNA levels were analyzed by qPCR. Mean values +/- SD are shown. (**e**) Electrophoretic mobility shift assay (EMSA) analysis using a conserved PDGFRB AP-1 site (PDGFRBAP-1) and a mutated version (PDGFRBAP-1 mut). Depletion of JunB and cJun using a mixture of monoclonal antibodies (AB) resulted in strong reduction of DNA binding. (**f**) Chromatin

Immunoprecipitation (ChIP) in the human cell line BJ-1 confirmed binding of JunB and cJun to the AP-1 consensus sequence in the PDGFRB locus (PDGFRB). Reduced binding was observed to a negative 3' control region ($PDGFRB^{neg}$) (n = 3). Mean values +/- SEM are shown. (**g**) The functionality of the AP-1 site for PDGFRB promoter regulation was demonstrated with a luciferase reporter assay. Jurkat lymphoma cells were transfected with the indicated vectors and subjected to OneGlo-luciferase assay after 36hrs. The promoter-less pGL3 luciferase vector was used as control. Cells were co-transfected with 0.05 µg p-ßGAL and subjected to a BetaGlo assay for normalization. Mean RLU levels +/- SD are shown (n = 3).

Figure 3. PDFGR inhibition interferes with formation of transplanted tumors. (**a**) Western Blot analysis for PDGFRB and PDGFRA expression in different murine cell lines isolated from *CD4*-NPM-ALK lymphomas. HSC-70 (HSPA8) was used as a loading control. (**b**) Tumor weight of transplanted *CD4*-NPM-ALK cell lines A333 (no PDGFRB expression; n = 4), MEL406 (intermediate PDGFRB expression; n = 4), and CD4-417 (high PDGFRB expression; n = 8) without (black circles) and with imatinib treatment (blue squares). The weight of tumors was determined 7 days after initiation of imatinib treatment. (**c**) Survival curves of untreated and imatinib-treated *CD4*-NPM-ALK and *CD4*-NPM-ALK-$CD4^{\Delta\Delta Jun}$ mice. Treatment was started at 6 weeks of age and mice were sacrificed at 30 weeks of age. (**d**) Proliferation and apoptosis in transplanted CD4-417 lymphoma cells was assessed by Ki67- and TUNEL-staining. Representative images are shown. Bar graphs indicate the mean positive cell number (+/- SD) as determined by HistoQuest™ software (n = 5). (**e**) pPDGFRB expression levels in untreated (PBS) and imatinib-treated *CD4*-NPM-ALK mice. (**f**) Reduction of tumor size after treatment of MEL406-transplanted recipient mice with imatinib, crizotinib, or both. Mean tumor mass +/- SD is shown. (n = 10 mice per group). (**g**) Balb/c ALK^+ ALCL cells (VAC) were implanted into syngeneic Balb/c mice and treated with CEP28122 (100 mg/kg/bid). Tumors relapsed after 14 days of CEP28122 treatment and were then treated with CEP28122 + imatinib (start of treatment is indicated for each mouse by green arrowheads). (**h**) Balb/c mice were injected with syngenic ALK^+ ALCL cells. Animals with lymphomas larger than 1 cm in diameter were then treated with CEP28122 or CEP28122 + imatinib. Data from individual mice are shown.

Figure 4. Complete remission of ALCL in a patient following imatinib treatment.
(a) Gene expression profiles obtained from three publicly available (GSE6338, GSE14879, GSE19069), proprietary, and unpublished datasets including PTCL, ALK^- and ALK^+ ALCL. Note the increased expression of JunB, cJun, genes encoding for Fos AP-1 members and PDGFRs. (b) Quantitation of immunohistochemistries for PDGFRA and PDGFRB on > 280

human PTCL/NOS, AITL, ALK$^+$ ALCL and ALK$^-$ ALCL tumor samples. In contrast to PTCL/NOS and AITL, ALCL patient samples displayed high expression of both, PDGFRA and B, in most cases. Number of cases with positive staining in italic / total number of cases per dataset in standard. The (**c**) H&E-staining and immunohistochmistry for indicated markers on tumor sections from a 27-year old patient with grade III ALK$^+$ ALCL that was refractory to standard treatment. (**d-g**) Imatinib treatment (400 mg/day) led to complete remission of ALCL in the patient. **(d)** Within 10 days of treatment, axillary lymph nodes (encircled with white dotted line) became PET-CT-negative. L, lung; H, heart; R, rib-cage. (**e,f**) The serum concentrations of tumor markers beta-2-microglobulin (B2M) and soluble CD30 (sTNFRSF8) as well as acute phase parameters haptoglobin (HP) and C-reactive protein (CRP) returned to normal levels after imatinib treatment. The transient increase of CRP around day 27 (e) was due to an infection of the patient. Normal ranges for B2M and HP serum concentrations are indicated by the light green and the light blue areas, respectively (f). (**g**) PDGFB was elevated in platelet-low plasma before treatment in the patient and reverted to normal levels (light area) as early as 10 days after initiation of imatinib therapy. The patient has remained tumor-free since 18 months.

Methods

Cell culture

Cell lines CD-4-4, CD-417, MEL406, VAC, bT02, A943 and A333 were isolated from *CD4*-NPM-ALK mice and seeded at 1x10^6 cells/ml in RPMI 1640 Medium supplemented with 10% FBS and antibiotics. Cell numbers were determined with an electronic cell counter (CASY-1, Schärfe-System).

Mice

Mice carrying the human *CD4*-NPM-ALK fusion-gene[4,14] were crossed with *CD4*-Cre mice[35], as well as floxed JunB and/or cJun mice[36,37]. The genetic background of these intercrosses was C57Bl/6xBalb/c. For the Kaplan-Meier curve, only isogenic littermates of the following genotypes were used: wild type control, *CD4*-NPM-ALK-JunB$^{flox/flox}$;cJun$^{flox/flox}$ (*CD4*-NPM-ALK), *CD4*-NPM-ALK-*CD4*-JunB$^{\Delta/\Delta}$;cJun$^{\Delta/+}$ (*CD4*-NPM-ALK-*CD4*$^{\Delta JunB}$), *CD4*-NPM-ALK-*CD4*-JunB$^{\Delta/+}$;cJun$^{\Delta/\Delta}$ (*CD4*-NPM-ALK-*CD4*$^{\Delta cJun}$) and *CD4*-NPM-ALK-*CD4*-JunB$^{\Delta/\Delta}$;cJun$^{\Delta/\Delta}$ (*CD4*-NPM-ALK-*CD4*$^{\Delta\Delta Jun}$) mice. Mice were kept in a specific-pathogen-free facility and all animal experiments were done in agreement with the ethical guidelines of the Medical University of Vienna.

Xenograft experiments

12 week old female SCID mice were subcutaneously implanted with 1-5x10^6 cells. After two weeks, tumors had grown to the size of <1.0 cm and mice received either 100-200 mg/kg/day imatinib, nilotinib, crizotinib (100 mg/kg/day), imatinib + crizotinib (33 mg/kg/day) or PBS for seven days by oral gavage.

Syngenic engraftment

1x10^6 Balb/c ALK^+ ALCL cells (VAC and bT02) were subcutaneously implanted into 4-6 week old syngeneic Balb/c recipients. Mice with tumor masses of <1.0 cm were treated with CEP28122 (100 mg/kg/bid), CEP28122 (100 mg/kg/bid) + imatinib (200 mg/kg/bid) or CEP28122 (100 mg/kg/bid) followed by CEP28122 (100 mg/kg/bid) + imatinib (200 mg/kg/bid).

Imatinib treatment *CD4*-NPM-ALK tumor bearing mice

CD4-NPM-ALK-positive mice were treated with imatinib between 6 and 30 weeks of age as described for xenograft experiments. All animal experiments were approved by the ethical committee for animal experiments of the Medical University of Vienna and the Federal Ministry of Science and Research of Austria (animal license numbers: BMWF-66.009/0139-C/GT/2007, BMWF-66.009/0092-II/10b/2009, BMWF-66.009/0137-II/10b/2010 and BMWF-66.009/0001-II/3b/2011).

Patient samples, treatment and blood testing

The ALCL patient was treated under supervision of the Department of Internal Medicine I and in agreement with the ethic committee of the Medical University of Vienna with 400 mg imatinib/day after receipt of informed consent. Plasma samples were analyzed for CRP and haptoglobin concentrations (nephelomteric assays). PDGFB, sCD30 (sTNFRSF8) and beta-2-microglobulin (B2M) plasma levels were quantified by commercially available ELISAs (ebioscience).

Immunohistochemistry and immunofluorescence

IHC- and IF-stainings were performed with formalin fixed paraffin embedded tissues after receipt of informed patient consent and in accordance with the declaration of Helsinki. Antibodies used were: anti-Ki67 (Novocastra, NCL-KI67-P), anti-PDGFRA (Neomarkers, RB-9027), anti-PDGFRB (Cell Signaling, #3169), anti-pPDGFRB (SCBT, sc-12909), anti-Cleaved Caspase 3 (Cell Signaling, #9661), anti-Stat3 (SCBT, sc-7179), anti-p-Stat3 (Cell Signaling, #9145), anti-p-Akt (Cell Signaling, #3787), anti-JunB (SCBT, sc-46), anti-cJun (SCBT, sc-1694), anti-cJun (Cell Signaling, #9165), anti-ALK (Zymed, 51-3900), anti-CD30 (DAKO, M0751), anti-CD31 (Dianova, DIA 310), anti-S100A/B (Dako, Z0311), anti-Collagen

IV (Chemicon, AB756P), anti-smooth muscle actin (Neomarkers, MS-113), anti-Vimentin (Abcam, AB28028). TUNEL-staining was performed with the "*in situ* cell death detection kit" (Roche) according to the manufacturers instructions. Images were captured with a Zeiss AxioImager Z1 microscope and quantified using HistoQuest™ and TissueQuest™ software (TissueGnostics GmbH, Vienna, Austria, www.tissuegnostics.com).

ChIP (Chromatin Immunoprecipitation)

Conserved AP-1 binding sites within the PDGFRB promoter were identified using the ecr browser (http://ecrbrowser.dcode.org)[38]. ChIP was performed as described[39]. 10^7 cells (CD4-417; BJ-1) or 100 µg of tumor tissue (*CD4*-NPM-ALK or *CD4*-NPM-ALK$^{\Delta/\Delta Jun}$ lymphomas) were used with anti-JunB sc-73X, anti-cJun sc-1694X and control antibodies (normal rabbit IgG, Santa Cruz). Primer sequences amplifying a conserved AP-1 binding site in the proximal murine PDGFRB promoter were: muPDGFRB-FW: 5'-CTCCATTTGACAGGCATCAG-3'; muPDGFRB-Rev: 5'-CTTCCTCCTTTCCCTCTGCT-3'. For negative control muPDGFRBneg-FW: 5'-TAGGCTGAGCAGGTCAACT-3'; muPDGFRBneg-Rev: 5'-TGTGCTCAGGGAGATGACAG-3' and for positive control muVEGF-FW: 5'-AATGGGATCCTCTGGGAAGT-3' and muVEGF-Rev: 5'-CACAGTGCATACGTGGGTTT-3' primers were used. For the human PDGFRB promoter, primer sequences were: huPDGFRB-FW: 5'-CAGGTCATCTGCTCCAAGTG-3' and huPDGFRB-Rev: 5'-TTGCACTGTCCTGTCTGTCC-3' as well as huPDGFRBneg-FW: 5'-GGGTATATGGCCTTGCTTCA-3' and huPDGFRBneg-Rev: 5'-GAGGAATCCCTCACCCTCTC-3' for negative control.

Promoter analysis and reporter gene assays

The "UCSC Genome Browser on Mouse, July 2007"[15] and "MathInspector"[16] were used for *in silico* promoter analysis. Luciferase assays were performed as previously described[40]. PDGFRB-luc and PDGFRBΔ(-w/o AP-1 site)-luc pGL3 vectors (Promega) were cloned by PCR. Human cJun and JunB pCDNA3.1 (Invitrogen) expression vectors were used together with a beta-gal control vector (pMIR-REPORT; Ambion) for relative luciferase quantification.

Electromobility shift Assay (EMSA)

Oligonucleotides were annealed at equimolar concentrations (40 µM) in 200 µl annealing buffer (0.0625 x PCR buffer II Roche; 0.94 M $MgCl_2$). For supershift reactions, 2 µg of antibodies specific for JUNB and JUN (anti-JunB sc-73X, anti-cJun sc-1694X) were used.

Gene expression profiling

The gene expression data were obtained from three publicly available (GSE6338,

GSE14879, GSE19069 at NCBI GEO repository http://www.ncbi.nlm.nih.gov/geo/)[31-33], proprietary[34], and unpublished datasets including T cells from ALCL, PTCL. Expression values were extracted from CEL files and normalized with RMA Selected probe lists were visualized in a heat map format using Heat Map Viewer available as a GenePattern module.

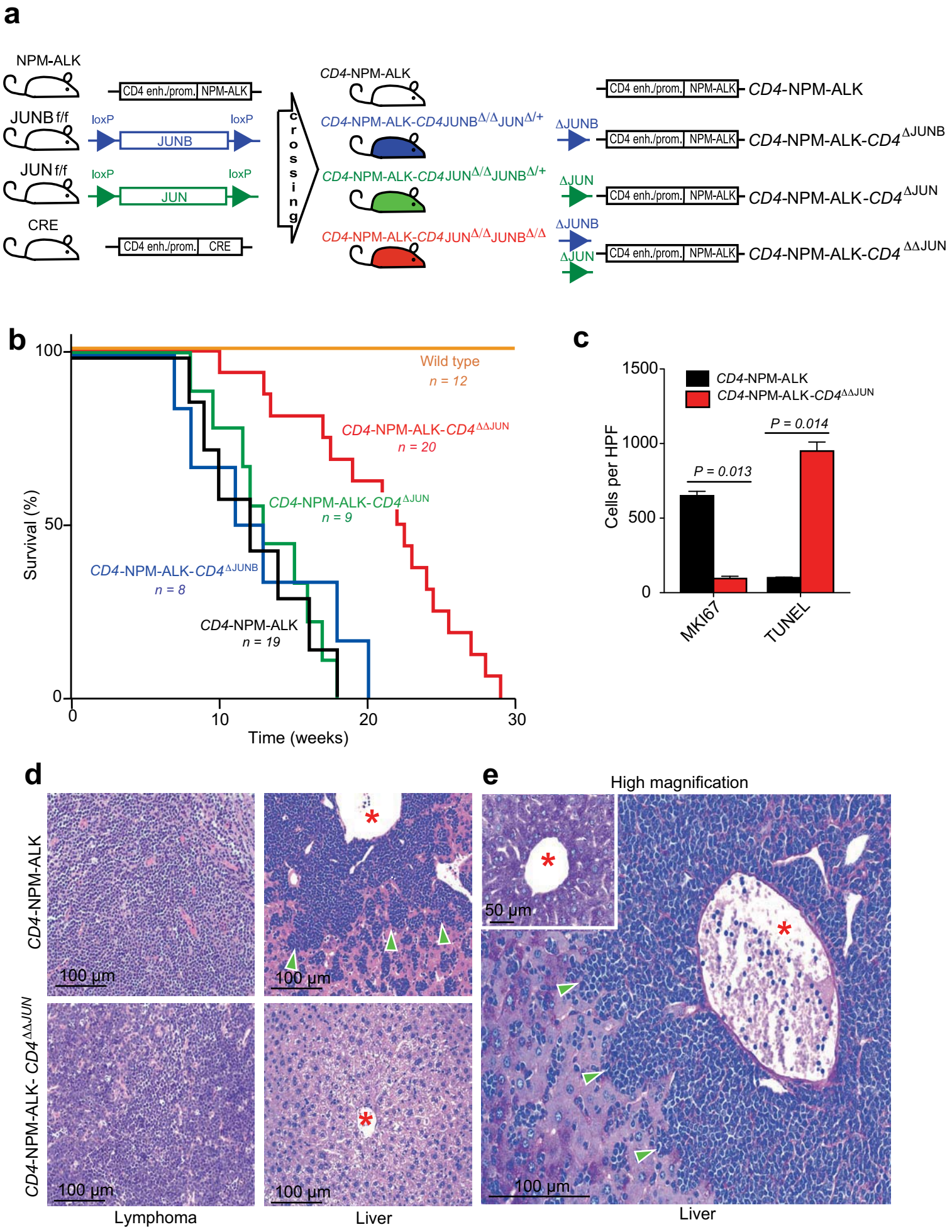

Laimer et al. Figure 1

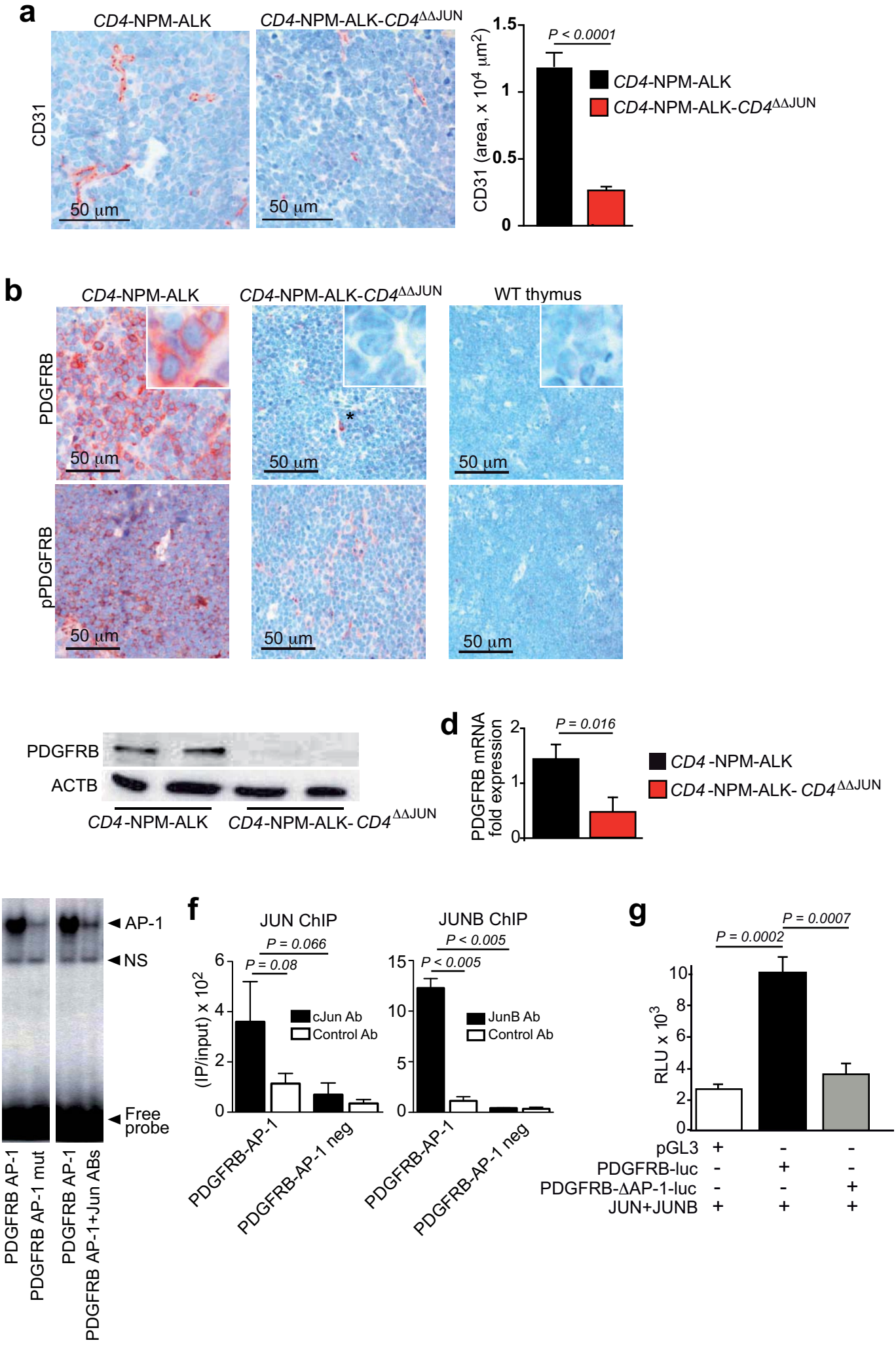

Laimer et al. Figure 2

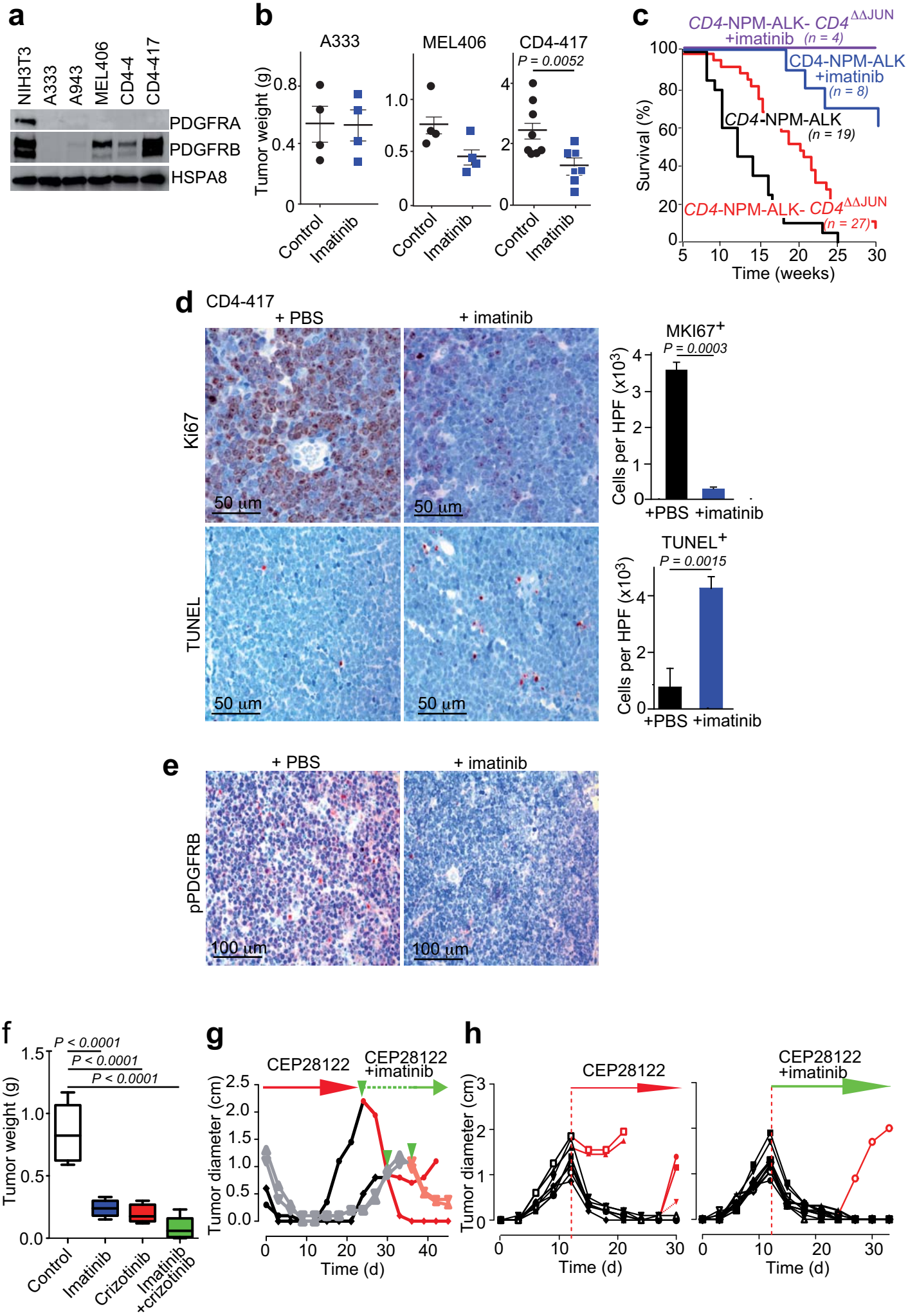

Laimer et al. Figure 3

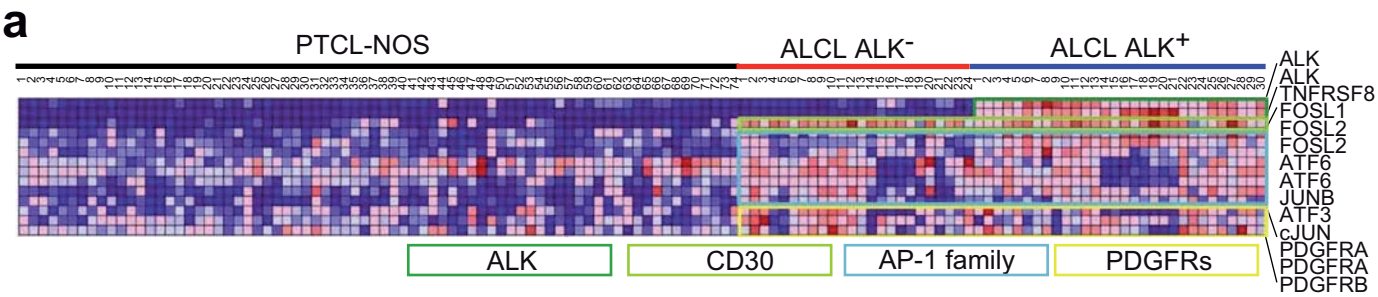

b

TCL subtype	***PDGFRA*** *positives*/sample set	***PDGFRB*** *positives*/sample set
PTCL/NOS	*128*/141	*4*/38
AITL	*36*/36	*0*/15
ALCL ALK+	*77*/79	*53*/71
ALCL ALK-	*31*/31	*33*/48